

3D-Printed Biomimetic Cervical Vertebral Body for Spinal Arthroplasty Testing

Jenna M. Wahbeh, M.S.^{1,2}; Erika Hookasian, B.S.^{1,2}; John Lama, B.S.^{1,2}; Labiba Alam, B.S.^{1,2};
Sang-Hyun Park, Ph.D.^{1,3}; Edward Ebramzadeh, Ph.D.^{1,3}; Sophia N. Sangiorgio, Ph.D.^{1,2,3}

¹The J. Vernon Luck, Sr., M.D. Orthopaedic Research Center Orthopaedic Institute for Children in Alliance with UCLA, Los Angeles, CA

²University of California Los Angeles, Department of Bioengineering, Los Angeles, CA

³University of Southern California, Department of Biomedical Engineering, Los Angeles, CA

DISCLOSURES: Jenna M. Wahbeh (N); Erika Hookasian (N); John Lama (N); Labiba Alam (N) Sang-Hyun Park (N); Edward Ebramzadeh (N); Sophia N. Sangiorgio (N)

INTRODUCTION: Cervical disc arthroplasty is a promising, motion-sparing, alternative to anterior cervical discectomy and fusion. Few biomechanical studies have been conducted to improve the preclinical assessment and clinical success of these implants. The paucity of cervical spine biomechanical testing may be due to the lack of biofidelic, reproducible cervical vertebral body models. Composite models have become commonplace for the assessment of fixation and stability of total joint replacements; however, there are no comparable models for the cervical spine, potentially due to the varying strengths of the vertebral body. The goal of this study was to create a tunable, customizable model of a cervical vertebra to assess cervical device performance.

METHODS: A comprehensive literature search was performed to identify an acceptable range of shear and compressive strength values for an expected range of cancellous bone strength in the cervical spine. Literature was identified that defined eleven unique vertebral regions of varying density, based on CT scan densities. Original calculations were performed to convert each bone density to compressive strength (Table 1). Using additive manufacturing software, rectangular prints with three lattice structures, gyroid, triangle, and zig-zag, and a range of in-fill densities, 5% to 100%, were 3D-printed. Following successful prints, each specimen was tested for coronal compressive strength and shear strength using a custom pure compression apparatus on a servo-hydraulic load. One print pattern was selected for material and structural properties and compressive and shear strength was evaluated in the sagittal plane. A best-fit relationship was then calculated for each lattice structure and density. This model was then validated through testing of in-fill densities that were chosen based on extrapolated values. Specifically, the calculated strength values were used to extrapolate specific in-fill densities. These densities were then tested under the same compression protocol to ensure a valid relationship between strength and in-fill density. Finally, a complete cervical vertebral model was created using specific in-fill densities and lattice structures that most closely matched the strength values in the specific regions.

RESULTS: Using the previously identified equations for relationships between bone density and compressive strength, the eleven unique regions were converted to compressive strength with values ranging from 9.3 to 61.2 MPa (Table 1). A linear relationship was identified through material testing between in-fill densities and strength for triangle and zig-zag lattice structures and an exponential relationship for gyroid lattice structures (Figure 1). The axial compressive strength of the gyroid specimens ranged from 1.5MPa at 10% infill to 31.3MPa at 100% infill and the triangle structure ranged from 2.7MPa at 10% infill to 58.4MPa at 100% infill. The gyroid specimens were tested in the coronal plane, as well, and compressive strength was found to be about 20% less than the compressive strength in the axial plane. Triangle and zig-zag specimens buckled at failure while gyroid specimens were crushed, similar to the failure pattern observed in cancellous bone. Based on these results, a cervical vertebra model was made with eleven different in-fill densities ranging from 33% gyroid to 84% triangle. Following the mathematical best-fit relationships and comparison to the calculated strength values, a computer model of the C5 vertebra was created with nTopology software. This model was constructed with 11 specific anatomical regions available for customizations. Finally, one C5 cervical vertebral body model, using the previously calculated strength values and correlated in-fill densities, was 3D-printed to ensure a seamless design of the non-homogenous regions (Figure 2).

DISCUSSION: This study shows the successful use of additive manufacturing techniques and materials to recreate material properties of cancellous bone in the vertebral body. As the cervical spine has varying compressive strengths from the lateral edges to the central portions and around the pedicles, a completely customizable model with varying strengths may be more clinically relevant for biomechanical testing. The iterations from the current study are necessary to ensure a close match to the cancellous bone material. The findings from the present study introduced a framework for using additive manufacturing to create a tunable, customizable biomimetic model of a cervical vertebra. This model may provide a useful tool for a more comprehensive and efficient approach to the preclinical evaluation of cervical disc replacements.

SIGNIFICANCE/CLINICAL RELEVANCE: To our knowledge, the present study introduces the first framework for using additive manufacturing to create a tunable, customizable biomimetic model of a cervical vertebral body. This model may provide a useful tool for a more comprehensive and efficient approach to the preclinical evaluation of cervical disc replacements.

TABLES AND FIGURES:

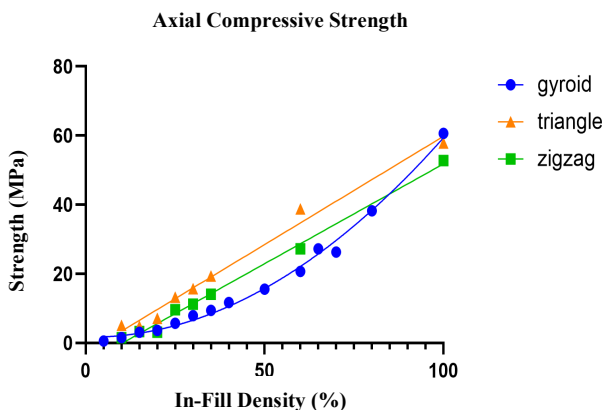


Figure 1 Measured Axial Compressive Strength for Each Lattice Structure with best-fit model for each.

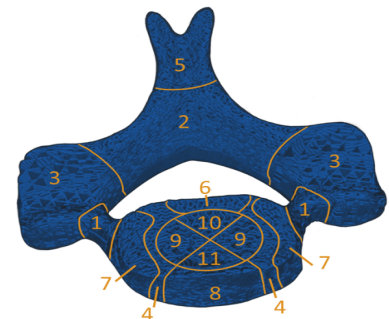


Figure 2. Final model created with altering in-fill densities

Table 1. Regions of Cervical Cancellous Bone, Respective Density, and original strength calculations

Region	Density (mg/cc)	Strength (MPa) via Lang et al	Strength (MPa) via McBroom et al
Pedicle (1)	630	59.3	61.2
Lamina (2)	555	43.5	46.0
Lateral Mass (3)	550	42.5	45.1
Exterior Body (4)	455	26.8	29.4
Spinous Process (5)	430	23.3	25.8
Exterior Body (Posterior) (6)	415	21.4	23.8
Uncinate Process (7)	410	20.7	23.2
Exterior Body (Anterior) (8)	370	16.2	18.4
Central Body (Lateral) (9)	355	14.6	16.8
Central Body (Posterior) (10)	350	14.1	16.2
Central Body (Anterior) (11)	295	9.3	11.0